

send to Serena, Saul, Tony

Saul's comments

Restframe *I*-band Hubble diagram for Type Ia supernovae

S. Nobili¹, R. Amanullah¹, G. Garavini¹, A. Goobar¹, C. Lidman², V. Stanishev¹, and ...THE SUPERNOVA COSMOLOGY PROJECT

¹ Department of Physics, Stockholm University,
AlbaNova University Center, S-106 91 Stockholm, Sweden

² ...

Received ...; accepted ...

Abstract. Using a novel technique for fitting restframe *I*-band lightcurves of Type Ia supernovae, a Hubble diagram including 28 SNe with $0.01 < z < 0.1$ was constructed. Adding three SNe at $z \sim 0.5$ yields results compatible with the expectations for a flat Λ -dominated “concordance universe” (Ω_M, Ω_Λ)=(0.3,0.7). The high-*z* supernova NIR data was also used to test for systematic effects in the use of SNIa as distance estimators. A flat, $\Lambda = 0$ universe where the faintness of supernovae at $z \sim 0.5$ is due to gray dust homogeneously distributed in the intergalactic medium is disfavored at the 90 % confidence level based on the high-*z* Hubble diagram using this preliminary data-set. We also show that more supernovae are necessary to set limits on intergalactic dust based on *B-I* and *B-V* color measurements. The high-*z* restframe *I*-band lightcurves are fitted by templates that show a second peak, suggesting that they are not intrinsically subluminal.

Key words. cosmology: observations, supernovae: general

consistent

better fit by

than templates w/o a 2nd peak.

1. Introduction

Observations of type Ia supernovae (SNe) in restframe *B*-band up to redshifts 1 and above have shown that they are significantly dimmer than expected in a universe without a cosmological constant or some other form of dark energy (Riess et al., 1998; Perlmutter et al., 1999; Tonry et al., 2003; Knop et al., 2003). The evidence for dark energy is supported by cross-cutting cosmological results, such as the measurement of the cosmic microwave background anisotropy, which indicates a flat universe (De Bernardis et al., 2000; Jaffe et al., 2001; Sievers et al., 2003; Spergel et al., 2003); the evolution in the number density of X-ray emitting galaxy clusters (Borgani et al., 2001; Henry, 2001) and galaxy redshift surveys (Efsthathiou et al., 2002), the two latter indicate that $\Omega_M \approx 0.3$. Taken together, these independent measurements suggest a concordance universe (Ω_M, Ω_Λ)=(0.3,0.7). However, the SN Hubble diagram remains the most direct approach currently in use for studying cosmic acceleration and, thus, systematic effects affecting the observed brightness, of type Ia supernovae should be carefully considered. These include: uncorrected host galaxy extinction (Rowan-Robinson, 2002), dimming by photon-axion mixing over cosmological distances (Csaki et al., 2001; Deffayet et al., 2001; Mörtzell et al., 2002), dimming by intergalactic gray dust (Aguirre, 1999a,b) and intrinsic luminosity evolution (Drell et al., 2000).

Perlmutter et al 1998
Goobar et al 1998

advantages, e.g. less sensitivity to dust along the line of sight, either in the host galaxy or in the intergalactic medium. On the other hand, the “standard candle” properties at these wavelengths and the possibility of additional systematic effects need to be investigated.

For example,

Using restframe *I*-band, the uncertainty due to extinction by dust is greatly reduced as compared with restframe *B*-band measurements. For Milky-Way type dust ($R_V = 3.1$) the ratio of extinction for the two bands is sizable, $A_B/A_I \sim 2$. In general, the extinction corrections become less sensitive to our knowledge of the intrinsic supernova colors and dust properties.

The *I*-band lightcurves typically show a second peak, 15-30 days after the initial one. It has been suggested that the intensity and time-difference between the first and second *I*-band peak are related to the intrinsic luminosity of the Type Ia SNe, appearing later and more evident for normal Type Ia and earlier and fainter for subluminal ones (Hamuy et al., 1996a). Thus, building *I*-band lightcurves for high-*z* supernovae offers a way to investigate the possibility of finding means for secondary calibration and to probe for brightness evolution of Type Ia supernovae.

Wang submitter

I don't understand this sentence
① why high z isn't this evidence for the same param?

The scope of this work is to test the feasibility of using restframe *I*-band for cosmological distance measurements using data available up to date, and suggest the importance of observing in this wavelength range for the future samples of SNe. For that purpose, we develop a template fitting technique to estimate the first (I_{max}) and second (I_{sec}) *I*-lightcurve peaks. I_{max} is used to build a SN Ia Hubble diagram reaching out to

Determining cosmological distances through Type Ia supernovae fluxes at longer restframe wavelengths offers potential

Send offprint requests to: S. Nobili, serena@physto.se

Add a ref to technique of Allen et al.

I'm not sure we want to mention, unless we explain why they are wrong.

$z \sim 0.5$. The properties of the second peak in the restframe *I*-band lightcurves are investigated. Furthermore, the additional color information is used to test extinction by non-conventional dust for three $z \sim 0.5$ supernovae.

2. *I*-band lightcurve fit

Nearby samples of Type Ia SNe show a very characteristic lightcurve in the *I*-band: a secondary peak appears about 15-30 days after maximum light. This distinctive feature varies in strength and position with respect to the primary maximum, and complicates the use of a one parameter template for lightcurve fitting, being either the stretch factor s or the decline rate Δm_{15} , which currently often applied to *B* and *V* band (see, e.g., Goldhaber et al. (2001), and Hamuy et al. (1996) for an example of the stretch factor approach).

We have developed a method for fitting *I*-band lightcurves using five free parameters. The underlying function is a combination of two standard *B*-band templates of Type Ia supernovae¹. Our fitting procedure can be summarized as follows: one *B*-band template is used to fit the time (t_1) and the first peak magnitude (I_1), together with a stretch factor (s_1), which is also applied to the second *B*-band template shifted in time to fit the time (t_2) and magnitude of the second peak (I_2). The five parameters fitted are thus: $\{t_1, t_2, I_1, I_2, s_1\}$, (see Table 1).

Contardo et al. (2000) proposed a model composed of as many as 4 functions for a total of 10 parameters in order to fit all *UBVRI*-bands. Their method used two Gaussian functions to fit the two peaks together with a straight line to fit the late time decline and an exponential factor for the pre-max rising part of the lightcurve. This method describes Type Ia SNe lightcurve in all optical bands, though, as the authors recognize, does not represent accurately the second peak in the *I*-band due to the influence of the linear decline. However, the main disadvantage of their method is the large number of free parameters, thus the need for the object to be extremely well sampled.

The use of the standard *B*-band template of Type Ia supernovae, reduces the number of free parameters by a factor of two. Moreover, with this choice, no additional functions are needed to fit the pre-max rising part of the lightcurve nor the late time decline. Implicitly, we have thus assumed that the rising part of the lightcurve in *I*-band is the same as in *B*-band. As our goal is only to measure the position and amplitude of the first two peaks, we limit the fit to 40 days after maximum, neglecting the late time decline. Note that, unless otherwise specified, the supernova phase always refers to the time of restframe *B*-band lightcurve maximum.

2.1. The data set

We applied this method to fit a sample of local SNe for which both *B* and *I*-band data are publicly available from the Calan/Tololo (Hamuy et al., 1996a), Cfa (Riess et al., 1999) and Cfa2 (Jha, 2002) data sets. Data from three other well studied individual supernovae were also included: SN 1989B (Wells et al., 1994), SN 1994D (Richmond et al., 1995) and one subluminoous supernova: SN 1991bg. There are at least two

¹ The *B*-band template in Nugent et al. (2003) has been used.

| | |
|-----------|--|
| t_1 | time of the peak of the first <i>B</i> template |
| I_1 | peak magnitude of the first <i>B</i> template |
| t_2 | time of the peak of the second <i>B</i> template |
| I_2 | peak magnitude of the second <i>B</i> template |
| s_1 | stretch factor of the time axis |
| t_{max} | time of the first <i>I</i> -lightcurve peak |
| I_{max} | first <i>I</i> -lightcurve peak magnitude |
| t_{sec} | time of the second <i>I</i> -lightcurve peak |
| I_{sec} | second <i>I</i> -lightcurve peak magnitude |

Table 1. Summary of the parameters used in this work to describe the *I*-band lightcurve. The first five parameters are determined by fitting the data (see text for details). The next four parameters are the actual time and peak values of the lightcurve. Note that $I_1 = I_{max}$ by construction.

available data sets in restframe *I*-band for SN 1991bg, one published by Filippenko et al. (1992) with quite good coverage from about 3 days after *B*-band maximum light to +60 days, another one published by Leibundgut et al. (1993) with four data points, the first of which is at the time of *B*-band maximum. The agreement between the two data sets was assessed by comparing the measurements taken at the same date, i.e. JD=2448607, where we found a difference of 0.06 mag. This was considered to be the uncertainty for the four data points from Leibundgut et al. (1993) since they scatter more and no error-bars were reported in the original paper.

2.2. Fitting results

Only supernovae with at least 6 data points and a coverage in time constraining both peaks, were selected for lightcurve fitting. This resulted in a total of 42 SNe. Table 2 lists the parameters resulting from the fitting procedure. Note that the fit was performed in units of flux, while the parameters given in the table are transformed in magnitudes. Prior to fitting, all data points were *K*-corrected to restframe *I*-band as in Kim et al. (1996), assuming standard Bessel *I*-band, using the spectral template in Nobili et al. (2003) and time information from the available *B*-band data. Note that the values of I_2 reported in Table 2 are not the actual magnitude of the secondary peak, I_{sec} , but the maximum of the second *B*-band template used to fit the second peak, while the fitted value of I_1 coincides with the maximum of the lightcurve, I_{max} . In general, $I = I_1 \mathcal{B}(t - t_1, s_1) + I_2 \mathcal{B}(t - t_2, s_1)$, where \mathcal{B} is the *B*-band lightcurve template.

A potential source of systematic uncertainties is in the *K*-corrections due to the wide Ca IR triplet absorption feature, found to vary considerably among Type Ia supernovae. However, up to $z \sim 0.1$ the contribution of this feature is in general not critical to the precision of the *K*-corrections. For more distant SNe this could be a source of systematic uncertainty that has to be taken into account.

Figures 1- 4 show all the fitted lightcurves, except for the two very subluminoous supernovae: SN 1991bg and one of the supernovae in the Cfa2 data-set: SN 1997cn, shown in Fig. 5. As no date of *B*-band maximum light is known from the source

The second light curve peaks seen in lighter color
Avoid repetition

Retain the data (1997 and)

Answer is in approach
has also been proposed by Wang (substantiated)
calls it "super-stretch"
no explosive
stretch - a good word

added to the first peak with a time delay to together

timescale for the stretch factor approach

Perhaps we need a separate statement to say how this and for all might handle 2nd peak

Spell out all 3 names of first reference to 3rd paper

No Mag et al reference to?

should both be [S1(t-t)

Is this discussed in Nugent et al?

literature?

of SN 1997cn, the origin of the time axis was put to the epoch ($JD = 2450597.75$) when this supernova was first observed. Note that the second peak for the sub-luminous supernovae is almost completely absent, resulting in a value of $I_{29} \sim 2.5$ to 3 magnitudes fainter than I_1 .

Our sample includes also SNe that are classified as spectroscopically peculiar, showing similarities with the over-luminous SN 1991T; (Li et al., 2001; Howell, 2001). These are SN 1995bd, SN 1997br, SN 1998ab, SN 1998es, SN 1999aa, SN 1999ac, SN 1999dq and SN 1999gp. However, these do not show special peculiarities in their *I*-band lightcurve shape when compared to spectroscopically normals.

Analyzing the results of our fits, we found that Type Ia SNe show a variety of properties for the *I*-band lightcurve shape. In particular we noticed that the lightcurve could peak between -3 days and +4 days w.r.t B_{max} , as shown in Figure 6 (left panel). The time of the second peak, t_{sec} (relative to B_{max}), is shown in the right panel. The distribution of t_{max} is centered at day -0.9 and has a dispersion of $\sigma = 1.6$ days. t_{sec} is centered at 23.6 with a dispersion of $\sigma = 4.1$ days.

The reduced χ^2 for the fits given in Table 2 are generally around unity, except for a few cases. In particular we note the case of SN 1994D that has a $\chi^2/dof \sim 26$. The uncertainties for this supernova may be underestimated. But, even assuming them to be of the order of a few percent (see Knop et al. (2003)), the reduced χ^2 remained large, possibly indicating the limitations of the fitting template. As in several other cases we find a systematic trend in the residuals, especially in the rising part of the lightcurves. *that suggest this fitting model or the B template used is not complete*

While the χ^2 gives a measurement of the goodness of the fit, in the next section we test the robustness and accuracy of the parameter estimation in our fitting method, reported in Table 2.

2.3. Monte-Carlo tests of the fitting method

Given the heterogeneous origin of the data sample, the quality and the sampling of the individual SN lightcurves vary considerably. Only a few supernovae have excellent time coverage in the *I*-band lightcurves, resulting in a wide range of accuracy in the fitted parameters. The robustness of the fitting procedure was tested for all circumstances of data quality and time sampling in our sample by means of Monte Carlo simulations. We generated 1000 sets of simulated lightcurves for each supernova. The synthetic data points had the same time sampling as the real lightcurves and with deviations from the best fit template by randomization according to the measurement errors (assumed Gaussian). The simulated lightcurves were fitted using the same method as for the experimental data sets. The distribution of the fitted parameters on the simulated data was used to compare with the input data from the fits of the experimental data. The mean value in the distribution of each parameter coincide generally with the one expected within one standard deviation, not giving evidence for biases. This lends confidence that the fitting procedure is robust, and given the model of the lightcurve template will not yield biased estimations of the parameters. However, on a total of 42 supernovae, 2 cases showed significant deviations.

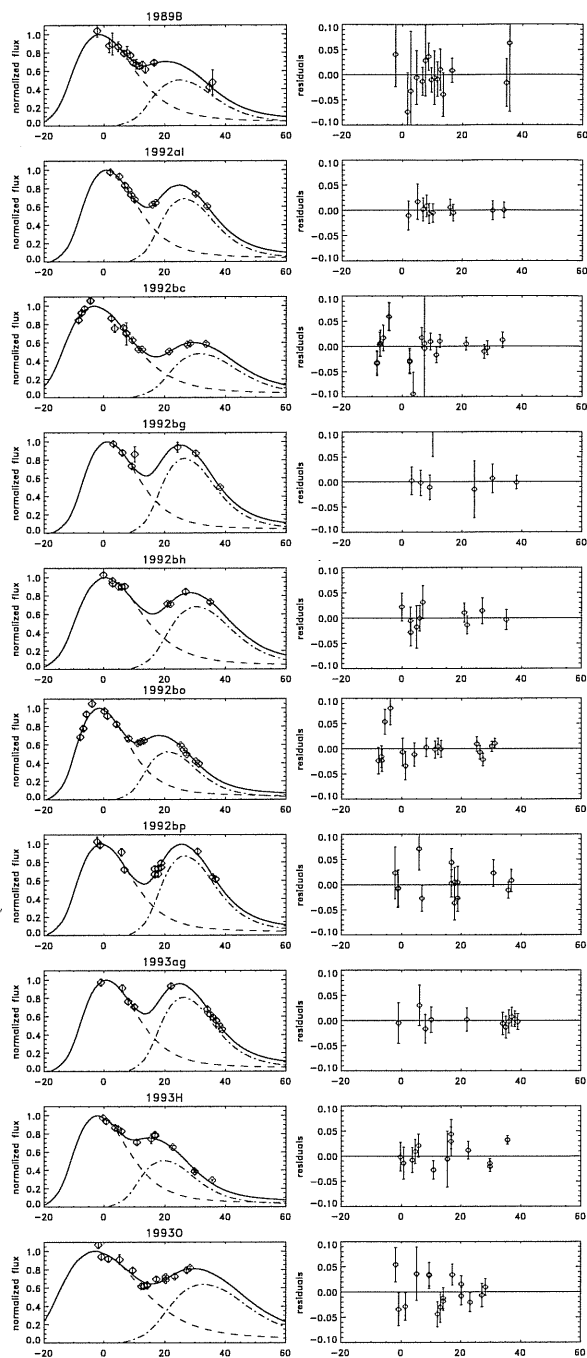


Fig. 1. *I*-band lightcurve fits. On the ordinate is the normalized flux, on the abscissa the restframe time since *B*-band maximum. The dashed line and the dash-dotted line represent the two *B*-band templates used to fit the first and second peak respectively.

- SN 1997br: in about 3% of the cases we found $\chi^2/dof \geq 7$. These cause the distributions to have different standard deviation than what is computed as uncertainty by the fitting procedure. Excluding them results in the expected distributions.
- SN 1998ab: the simulated data sets result in two populations of parameters, which reduces to one when imposing a

| SN | z | s_I | t_1 | I_1 | t_2 | I_2 | χ^2/dof |
|---------------------|-------|---------------|----------------|----------------|----------------|----------------|--------------|
| 1989B ¹ | 0.002 | 1.104 ± 0.122 | -0.710 ± 1.492 | 11.753 ± 0.056 | 23.029 ± 2.045 | 12.507 ± 0.164 | 0.52 |
| 1991bg ⁴ | 0.005 | 1.086 ± 0.035 | 3.668 ± 0.409 | 13.539 ± 0.006 | 28.896 ± 0.938 | 16.432 ± 0.128 | 1.46 |
| 1992al ⁴ | 0.015 | 0.958 ± 0.058 | 1.393 ± 1.121 | 15.096 ± 0.045 | 27.714 ± 1.182 | 15.505 ± 0.071 | 0.19 |
| 1992bc ⁴ | 0.020 | 1.175 ± 0.036 | -1.946 ± 0.177 | 15.686 ± 0.014 | 27.021 ± 0.529 | 16.486 ± 0.026 | 1.73 |
| 1992bg ⁴ | 0.035 | 0.935 ± 0.069 | 1.846 ± 1.814 | 17.707 ± 0.062 | 28.000 ± 2.855 | 17.928 ± 0.056 | 1.44 |
| 1992bh ⁴ | 0.045 | 1.102 ± 0.116 | 1.000 ± 1.045 | 18.065 ± 0.028 | 27.003 ± 1.872 | 18.482 ± 0.079 | 0.82 |
| 1992bo ⁴ | 0.019 | 0.897 ± 0.023 | -1.082 ± 0.177 | 16.095 ± 0.018 | 23.677 ± 0.391 | 16.801 ± 0.047 | 1.68 |
| 1992bp ⁴ | 0.079 | 0.910 ± 0.050 | -0.254 ± 0.832 | 19.110 ± 0.034 | 27.556 ± 1.174 | 19.264 ± 0.071 | 1.15 |
| 1993ag ⁴ | 0.049 | 0.931 ± 0.065 | 1.391 ± 0.983 | 18.504 ± 0.043 | 27.393 ± 2.224 | 18.735 ± 0.060 | 0.24 |
| 1993H ⁴ | 0.024 | 0.963 ± 0.035 | -1.563 ± 1.108 | 16.775 ± 0.044 | 20.594 ± 0.983 | 17.514 ± 0.051 | 3.42 |
| 1993O ⁴ | 0.051 | 1.358 ± 0.178 | -1.401 ± 1.688 | 18.318 ± 0.047 | 23.514 ± 1.509 | 18.804 ± 0.041 | 1.82 |
| 1994ae ³ | 0.004 | 1.052 ± 0.018 | -1.114 ± 0.143 | 13.396 ± 0.018 | 26.628 ± 0.329 | 14.025 ± 0.042 | 1.77 |
| 1994D ² | 0.002 | 0.891 ± 0.004 | -1.033 ± 0.043 | 12.182 ± 0.004 | 25.195 ± 0.090 | 12.833 ± 0.008 | 26.25 |
| 1994M ³ | 0.023 | 0.963 ± 0.038 | 0.183 ± 0.925 | 16.596 ± 0.038 | 24.487 ± 0.847 | 17.125 ± 0.061 | 3.14 |
| 1994T ³ | 0.035 | 0.750 ± 0.031 | 2.726 ± 1.659 | 17.570 ± 0.054 | 30.050 ± 1.229 | 17.820 ± 0.053 | 3.39 |
| 1995ai ³ | 0.005 | 1.171 ± 0.049 | -1.115 ± 0.494 | 13.539 ± 0.023 | 24.468 ± 0.761 | 14.151 ± 0.057 | 0.82 |
| 1995bd ³ | 0.016 | 1.211 ± 0.028 | -0.248 ± 0.120 | 16.135 ± 0.012 | 25.878 ± 0.347 | 16.626 ± 0.058 | 2.99 |
| 1995D ³ | 0.007 | 1.298 ± 0.063 | -1.677 ± 0.803 | 13.723 ± 0.031 | 24.336 ± 0.823 | 14.455 ± 0.039 | 0.52 |
| 1995E ³ | 0.012 | 1.049 ± 0.042 | -0.149 ± 0.676 | 15.427 ± 0.027 | 25.806 ± 0.959 | 16.090 ± 0.049 | 0.87 |
| 1996ai ³ | 0.003 | 1.114 ± 0.024 | -2.137 ± 0.554 | 13.991 ± 0.024 | 25.057 ± 0.510 | 14.667 ± 0.023 | 9.55 |
| 1996bi ³ | 0.036 | 0.976 ± 0.029 | 1.650 ± 0.423 | 17.165 ± 0.023 | 28.889 ± 0.729 | 17.683 ± 0.033 | 3.43 |
| 1996bo ³ | 0.017 | 1.262 ± 0.026 | -1.393 ± 0.156 | 15.757 ± 0.006 | 23.081 ± 0.210 | 16.228 ± 0.015 | 7.81 |
| 1996C ³ | 0.030 | 1.042 ± 0.046 | 2.247 ± 1.065 | 16.987 ± 0.036 | 28.164 ± 1.162 | 17.479 ± 0.034 | 4.40 |
| 1996X ³ | 0.007 | 1.114 ± 0.043 | -2.355 ± 0.369 | 13.412 ± 0.013 | 23.841 ± 0.750 | 14.180 ± 0.033 | 0.97 |
| 1997bp ⁵ | 0.008 | 1.234 ± 0.048 | 0.940 ± 0.302 | 14.164 ± 0.006 | 25.707 ± 0.507 | 14.622 ± 0.019 | 1.21 |
| 1997bq ⁵ | 0.009 | 1.003 ± 0.014 | 0.407 ± 0.098 | 14.587 ± 0.018 | 25.118 ± 0.237 | 15.135 ± 0.017 | 2.83 |
| 1997br ⁵ | 0.007 | 1.365 ± 0.038 | 0.636 ± 0.127 | 13.709 ± 0.022 | 20.375 ± 0.499 | 14.286 ± 0.037 | 3.08 |
| 1997cn ⁵ | 0.017 | 0.838 ± 0.054 | -1.271 ± 0.891 | 16.511 ± 0.030 | 24.217 ± 1.201 | 18.184 ± 0.158 | 1.42 |
| 1997dg ⁵ | 0.031 | 0.992 ± 0.057 | -1.126 ± 1.062 | 17.349 ± 0.037 | 26.103 ± 2.065 | 17.730 ± 0.050 | 4.14 |
| 1997E ⁵ | 0.013 | 0.960 ± 0.042 | -1.915 ± 0.336 | 15.511 ± 0.008 | 23.305 ± 0.403 | 16.058 ± 0.022 | 4.41 |
| 1998ab ⁵ | 0.027 | 1.493 ± 0.066 | -0.353 ± 0.334 | 16.573 ± 0.024 | 18.694 ± 0.701 | 17.012 ± 0.038 | 4.70 |
| 1998dh ⁵ | 0.009 | 1.003 ± 0.012 | -0.371 ± 0.174 | 14.114 ± 0.015 | 25.884 ± 0.284 | 14.678 ± 0.024 | 0.73 |
| 1998es ⁵ | 0.011 | 0.900 ± 0.106 | -3.022 ± 0.405 | 14.099 ± 0.016 | 24.657 ± 1.434 | 14.889 ± 0.073 | 0.82 |
| 1998V ⁵ | 0.018 | 0.941 ± 0.038 | 0.964 ± 0.685 | 15.866 ± 0.018 | 25.712 ± 0.758 | 16.073 ± 0.054 | 5.82 |
| 1999aa ⁵ | 0.014 | 1.325 ± 0.016 | 0.333 ± 0.079 | 15.284 ± 0.007 | 25.317 ± 0.187 | 15.845 ± 0.027 | 9.54 |
| 1999ac ⁵ | 0.009 | 1.230 ± 0.027 | 1.174 ± 0.311 | 14.354 ± 0.006 | 22.634 ± 0.486 | 15.045 ± 0.032 | 1.65 |
| 1999ci ⁵ | 0.008 | 0.992 ± 0.127 | -0.272 ± 0.545 | 13.165 ± 0.023 | 21.856 ± 1.195 | 13.698 ± 0.113 | 0.32 |
| 1999dq ⁵ | 0.014 | 1.213 ± 0.025 | -0.442 ± 0.127 | 14.833 ± 0.007 | 25.039 ± 0.209 | 15.300 ± 0.013 | 2.93 |
| 1999gp ⁵ | 0.027 | 1.331 ± 0.046 | -2.575 ± 0.278 | 16.448 ± 0.009 | 24.881 ± 0.507 | 17.007 ± 0.021 | 3.47 |
| 2000cn ⁵ | 0.023 | 0.769 ± 0.023 | -0.855 ± 0.198 | 16.721 ± 0.016 | 23.851 ± 0.381 | 17.198 ± 0.060 | 2.84 |
| 2000dk ⁵ | 0.017 | 0.840 ± 0.017 | -1.926 ± 0.209 | 15.811 ± 0.006 | 23.482 ± 0.409 | 16.259 ± 0.045 | 6.87 |
| 2000fa ⁵ | 0.021 | 1.131 ± 0.065 | -0.160 ± 0.351 | 16.353 ± 0.046 | 24.599 ± 0.544 | 16.845 ± 0.121 | 0.12 |

Table 2. Results of the *I*-band lightcurve fit of 42 nearby supernovae: t_1 and I_1 are the parameters for the time and amplitude fitted on the first *B*-band template, t_2 and I_2 are the parameters for the time and amplitude fitted on the second *B*-band template, and s_I is the stretch factor. The data were taken from: ¹ Wells et al. (1994); ² Richmond et al. (1995); ³ Riess et al. (1999); ⁴ Hamuy et al. (1996a); ⁵ Jha (2002); ⁶ Filippenko et al. (1992); Leibundgut et al. (1993).

cut on $\chi^2/dof \leq 6$. Note that about 78% of the simulations satisfy this condition.

In both cases a cut of the tail of the χ^2 distribution was enough to discriminate between the results, thus these supernovae were kept in the remaining analysis since the χ^2/dof of the fits to the real data fulfilled these criteria.

For the rest of the supernovae, the simulations confirmed the expected parameters, giving general confidence in the robustness of the procedure and the accuracy of the uncertainties on the parameters given in Table 2.

2.4. Intrinsic variations

Published *B*-band data was fitted using a template in order to determine the time of maximum luminosity, the stretch factor, s_B , and the amplitude of maximum, m_B , following Goldhaber et al. (2001). A width-luminosity relation was found for the first lightcurve peak. Figure 7 shows the *I*-band absolute magnitude versus the stretch factor in *B*-band for SNe with $z_{CMB} \geq 0.01$, where the distance to each SN was calculated from its redshift and assuming a value for the Hubble constant, $H_0 = 72 \text{ km s}^{-1} \text{ Mpc}^{-1}$, corrections for Milky Way and host galaxy extinction

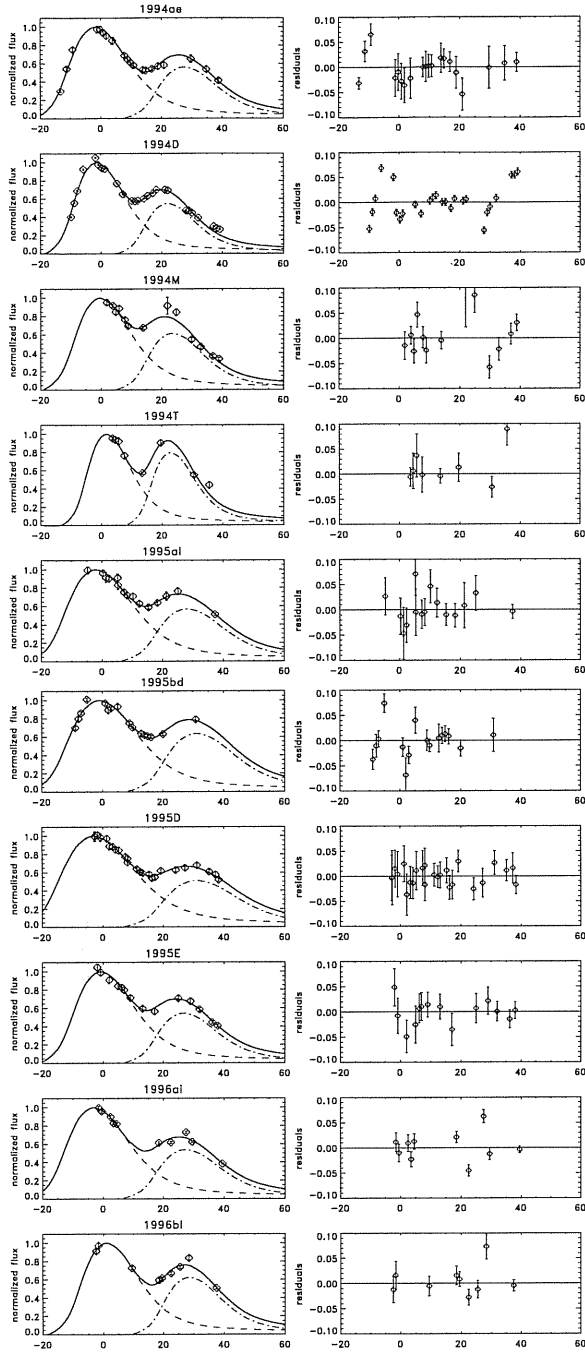


Fig. 2. I-band lightcurve fits. On the ordinate is the normalized flux, on the abscissa the restframe time since B-band maximum. The dashed line and the dash-dotted line represent the two B-band templates used to fit the first and second peak respectively.

were also applied, i.e.

$$M_{max}^I - 5 \log(H_0/72) = I_{max} - A_I^{MW} - A_I^{host} - 25 - 5 \log(d_L)$$

The error bars include an uncertainty of 300 km/s on the redshifts due to peculiar velocities of the host galaxies. The spread measured in the M_{max}^I is about 0.25 mag. The solid line shows the best fit to the data, obtained for a slope $\alpha_I = 1.13 \pm 0.19$ and

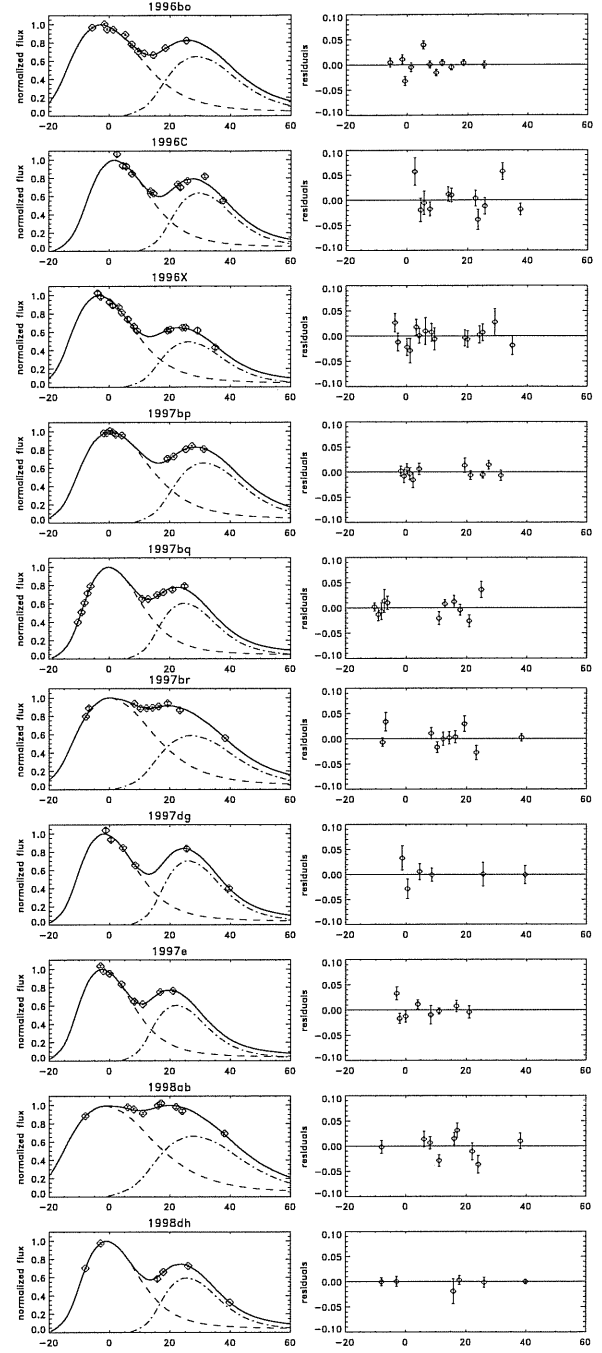


Fig. 3. I-band lightcurve fits. On the ordinate is the normalized flux, on the abscissa the restframe time since B-band maximum. The dashed line and the dash-dotted line represent the two B-band templates used to fit the first and second peak respectively.

an absolute magnitude for a stretch $s_B = 1$ supernova equal to $M_{max}^I(s_B = 1) = -18.74 \pm 0.03$ mag². The dispersion measured on the data along the fitted line is 0.19 ± 0.02 mag, considerably larger than what would be associated with mea-

² The value fitted for M_{max}^I depends on the value assumed for the Hubble parameter, $H_0 = 72$ km s⁻¹ Mpc⁻¹. However, its value is not used in any of the further analysis presented in this paper.

Note to discuss:
I believe this doesn't agree with other info on this

Is this the peak-to-peak spread or the RMS residual? say in text.

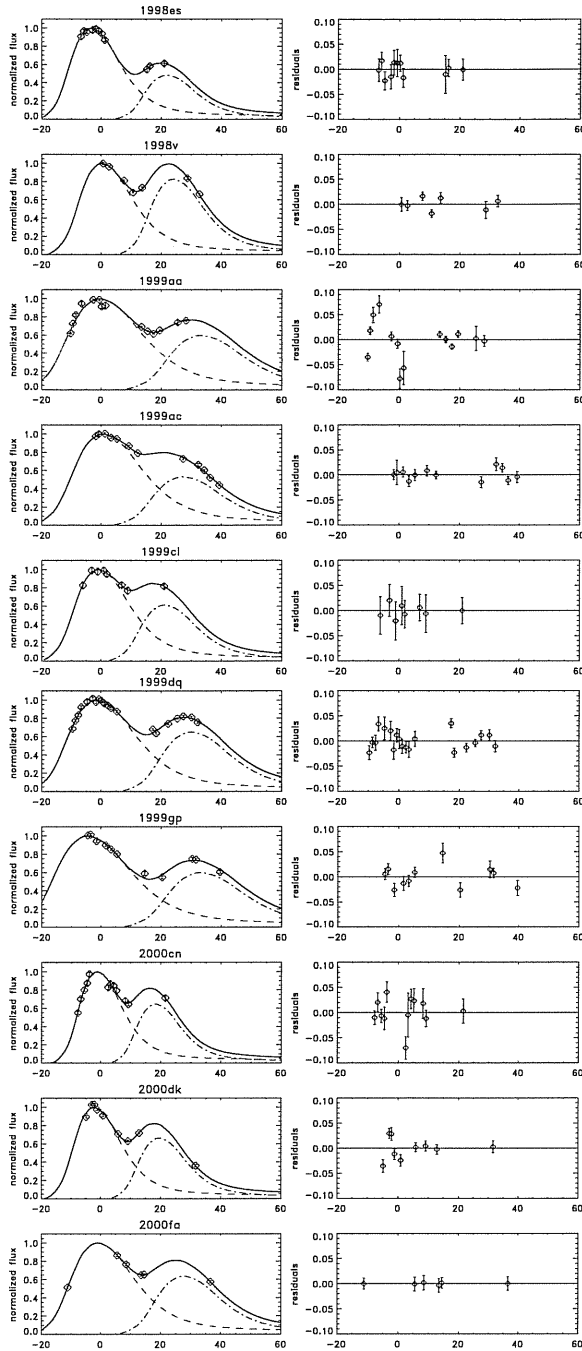


Fig. 4. *I*-band lightcurve fits. On the ordinate is the normalized flux, on the abscissa the restframe time since *B*-band maximum. The dashed line and the dash-dotted line represent the two *B*-band templates used to fit the first and second peak respectively.

surement errors. A more feeble correlation was found between the peak magnitude and the stretch in *I*-band, with a spread of about 0.22 mag. The host galaxy extinction corrections applied to most of the supernovae are those estimated by Phillips et al. (1999). The extinction for the supernovae in the CfA2 data set was calculated following the same procedure, using their *B* and *V*-band photometry. SN 1995E has been excluded

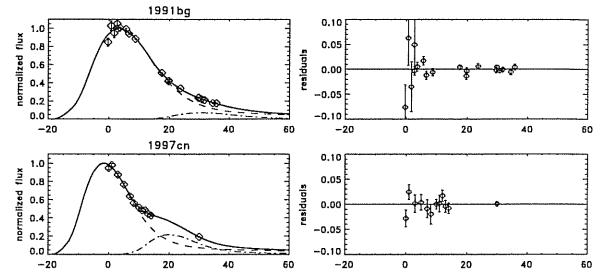


Fig. 5. *I*-band lightcurve fits of the under-luminous supernovae SN 1991bg and SN 1997cn. The dashed line and the dash-dotted line represent the two *B*-band templates used to fit the first and second peak respectively. Note that the second peak is fitted as ~ 3 mag fainter than the first peak.

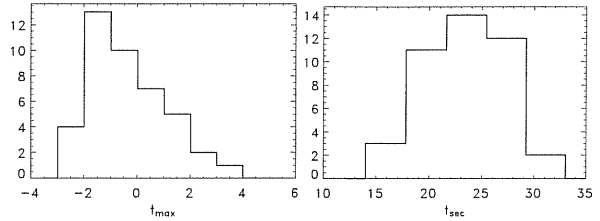


Fig. 6. Distribution of the time of *I*-band maximum referred to the time of *B*-band maximum (left panel) and the distribution of the time of second maximum referred to the time of *B*-band maximum (right panel).

from the sample as it is highly extinguished (see also discussion in Nobili et al. (2003)). No host-galaxy extinction corrections were made on SN 1998es and SN 1999dq as these two supernovae appear to be intrinsically redder than average, rather than reddened. Applying corrections based on average $B - V$ colors, would make these SNe deviantly bright in *I*-band compared to the rest of the sample.

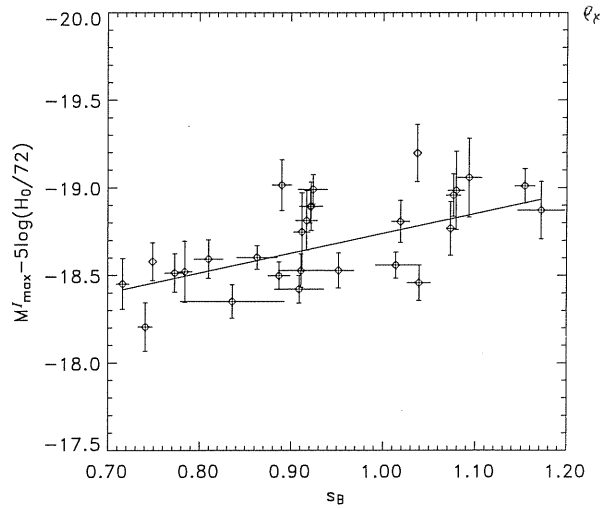


Fig. 7. *I*-band absolute magnitude versus stretch in *B*-band. The best fit gives $\alpha_1 = 1.13 \pm 0.19$ and $M_{max}^I(s_B = 1) = -18.74 \pm 0.03$ mag.

Should we first show s_B vs S_I plot?

A correlation was found between t_{sec} and the stretch factor both in B -, and I -band, as shown in Figure 8. There are a few outliers labeled in the figure, all of them but SN 1993H are identified as spectroscopically peculiar supernovae, (Li et al., 2001; Howell, 2001). However, other supernovae in our sample also classified as spectroscopically peculiar (by the same authors), behave as “normal” Type Ia SNe. A second order polynomial fits the data reasonably well, if the outliers are excluded.

Fig. 9 shows a possible correlation found between I_{sec} , corrected for the luminosity distance and both Galaxy and host galaxy extinction, and the stretch s_B , at least for $s_B < 1$. All of these correlations, shown in Fig. 7- 9, were expected since it has been suggested that the location and the intensity of the secondary peak depends on the B -band intrinsic luminosity of the supernova. *CITE?*

We have investigated the possible existence of further relations between the fitted parameters, but found no statistically significant correlations.

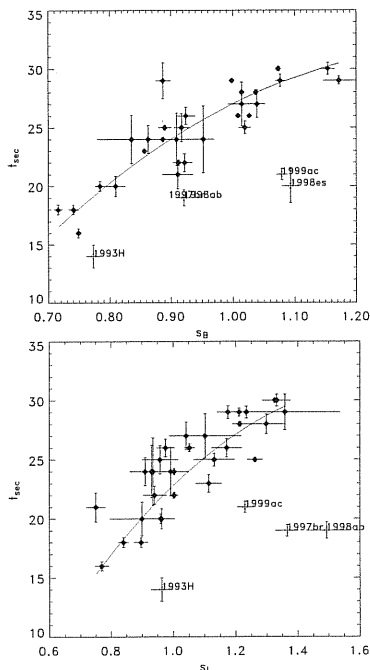


Fig. 8. Time of the second peak since B_{max} vs the stretch in B -band (top panel) and the stretch in I -band (bottom panel). A second order polynomial is fitted to the data excluding the labeled SNe.

3. The I -band Hubble Diagram

The fitted values of I_{max} , were used to build a Hubble diagram in I -band. A total of 28 supernovae of the sample considered here, are in the Hubble flow having a redshift $z_{CMB} \geq 0.01$. The whole redshift range spans up to 0.1.

The width-luminosity relation found between the fitted absolute I band magnitude and the B -band stretch factor was used to correct the peak magnitude, with a $\alpha_I = 1.13 \pm 0.19$ as measured in the previous section, similarly to what is usually done

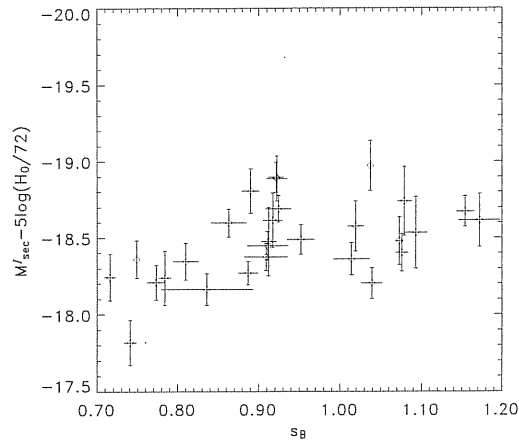


Fig. 9. Absolute magnitude of the secondary peak versus the stretch in B -band.

| SN | s_B | z_{CMB} | m_I^{eff} |
|--------|-------------------|-----------|--------------------|
| 1992al | 0.917 ± 0.012 | 0.014 | 14.922 ± 0.050 |
| 1992bc | 1.076 ± 0.008 | 0.020 | 15.732 ± 0.022 |
| 1992bg | 0.952 ± 0.017 | 0.036 | 17.297 ± 0.066 |
| 1992bh | 1.014 ± 0.022 | 0.045 | 17.822 ± 0.038 |
| 1992bo | 0.741 ± 0.008 | 0.017 | 15.753 ± 0.054 |
| 1992bp | 0.863 ± 0.022 | 0.079 | 18.829 ± 0.050 |
| 1993H | 0.773 ± 0.011 | 0.025 | 16.318 ± 0.063 |
| 1993O | 0.887 ± 0.012 | 0.053 | 18.094 ± 0.054 |
| 1993ag | 0.909 ± 0.027 | 0.050 | 18.069 ± 0.056 |
| 1994M | 0.810 ± 0.016 | 0.024 | 16.191 ± 0.056 |
| 1994T | 0.911 ± 0.025 | 0.036 | 17.253 ± 0.063 |
| 1995bd | 1.172 ± 0.026 | 0.014 | 15.152 ± 0.046 |
| 1996C | 1.039 ± 0.013 | 0.027 | 16.842 ± 0.040 |
| 1996bl | 0.924 ± 0.016 | 0.035 | 16.742 ± 0.033 |
| 1996bo | 0.890 ± 0.011 | 0.016 | 14.980 ± 0.025 |
| 1997bq | 0.912 ± 0.009 | 0.010 | 14.252 ± 0.027 |
| 1997dg | 0.836 ± 0.057 | 0.030 | 16.948 ± 0.081 |
| 1997E | 0.784 ± 0.008 | 0.013 | 14.903 ± 0.043 |
| 1998ab | 0.921 ± 0.010 | 0.028 | 16.352 ± 0.031 |
| 1998es | 1.093 ± 0.014 | 0.010 | 14.146 ± 0.029 |
| 1998V | 0.922 ± 0.013 | 0.017 | 15.269 ± 0.028 |
| 1999aa | 1.073 ± 0.005 | 0.015 | 15.294 ± 0.017 |
| 1999ac | 1.079 ± 0.009 | 0.010 | 14.204 ± 0.019 |
| 1999dq | 1.037 ± 0.000 | 0.014 | 14.675 ± 0.010 |
| 1999gp | 1.154 ± 0.011 | 0.026 | 16.337 ± 0.033 |
| 2000cn | 0.749 ± 0.000 | 0.023 | 16.045 ± 0.051 |
| 2000dk | 0.716 ± 0.007 | 0.016 | 15.347 ± 0.055 |
| 2000fa | 1.019 ± 0.010 | 0.022 | 16.025 ± 0.048 |

Table 3. List of SNe used in the Hubble diagram. m_I^{eff} is the peak magnitude corrected for the dust extinction and for the width-luminosity relation, following Eq. 1.

in B -band (Perlmutter et al., 1999). The peak magnitude was also corrected for Milky Way and for host galaxy extinction:

$$m_I^{eff} = m_I + \alpha_I(s_B - 1) - A_I^{host} - A_I^{MW} \quad (1)$$

The effective magnitude, m_I^{eff} for the nearby supernovae, listed in Table 3, have been used for building the Hubble diagram in I -band, shown in Figure 10. The estimated intrinsic uncertainty

This is a change from the usual definition. We can't just ignore the change in explanation.

Is this $0.19^2 - 0.02^2 \approx 0.19^2$ (i.e., after subtracting off measurement error?)
 Nobili et al.: Restframe I-band Hubble diagram for Type Ia supernovae

of 0.19 mag has been added in quadrature to the error bars of the plotted data. The solid line represent the best fit to the data for the concordance model $\Omega_M = 0.3$ and $\Omega_\Lambda = 0.7$. The fitted parameter, M_I , is defined as: (as in Perlmutter, 1997) to be

$$M_I \equiv M_I - 5 \log H_0 + 25 \quad (2)$$

where M_I is the I-band absolute magnitude for a B-band stretch $s_B = 1$ supernova. The value fitted is $M_I = -3.11 \pm 0.04$, $\chi^2 = 24.91$ for 27 degrees of freedom. Note that if no correction $\alpha_I(s_B - 1)$ is applied the dispersion in the Hubble diagram becomes 0.24 ± 0.02 mag, smaller than the corresponding dispersion (~ 0.4 mag) measured in the "uncorrected" B-band Hubble diagram. The ^{I-band} found dispersion (0.19 mag) is larger than the estimate given by Hamuy et al. (1996b) (~ 0.13 mag) using 26 SNe of the Calan/Tololo sample. For this reason we tried to compute the r.m.s. in the Hubble diagram for the three data set separately. We found the dispersion in the 9 SNe of the Calan/Tololo sample to be 0.15 ± 0.02 mag, in agreement with the result by Hamuy et al. (1996b). The same dispersion was measured in the CfA2 sample, while a significantly larger dispersion was found in the the CfA sample (see Table 4), although it includes supernovae in the same redshift range. We also note that the χ^2 of the lightcurve fits for these SNe is comparable to the other data-sets. Possible sources of the larger dispersion may include systematic effects in the MW and host galaxy extinction corrections and in the absolute I-band flux calibration. Differences in the instrumental set-ups may also be important. For all of the CfA sample and the CfA2 supernovae prior to December 98 a broader I-band filter reaching beyond $1 \mu\text{m}$ was used, i.e. about 900 \AA redder than edge of the Bessel I-band transmission curve.

Still need to understand if and why this is worse than Kassin's and if it were seeing.

| sample | n | σ |
|--------------|----|-----------------|
| Calan/Tololo | 9 | 0.15 ± 0.02 |
| CfA | 6 | 0.28 ± 0.04 |
| CfA2 | 13 | 0.15 ± 0.03 |

Table 4. Dispersion measured in the Hubble diagram for each of the sample, corrected for the width-luminosity relation; n is the number of data points; σ is a simple r.m.s. about the best fit model.

4. High redshift supernovae

Next, we explore the possibility of extending the Hubble diagram to higher redshifts, where the effects of the energy density components are, in principle, measurable. The restframe I-band data available up to date for this purpose is unfortunately very limited. It consists of only three supernovae at redshift $z \sim 0.5$ observed in the near infrared (NIR) J-band collected during three different campaigns conducted using different facilities and by two different teams. Keeping all of these sources of systematic errors in mind, we include the three supernovae in the Hubble diagram to show its potential and complementarity with respect to the standard B-band Hubble diagram.

The following sections describe the three high-z supernovae, SN2000fr, SN1999ff and SN1999Q, and the lightcurve fitting procedure used.

4.1. SN 2000fr

SN 2000fr was discovered by the Supernova Cosmology Project (SCP) during a search for type Ia supernovae at redshift $z \sim 1$ conducted in I-band with the CFH-12k camera on the Canada-France-Hawaii Telescope (CFHT). The depth of the search allowed us to discover this supernova during its rise time about 11 rest-frame days before maximum B-band light.

The supernova type was confirmed with two spectra taken at the Keck II telescope and VLT, showing that it was a normal type Ia at $z = 0.543$, see Garavini et al. (2003) for an extensive analysis of the spectra. The early discovery allowed to initiate an extensive follow-up program in restframe B, V and I filters involving ground and space based facilities. Approximately one year later, when SN2000fr had sufficiently faded, infrared and optical reference images were taken. The optical lightcurve has been fitted, yielding a stretch parameter $s_B = 1.064 \pm 0.011$ (Knop et al., 2003). Using restframe B - V measurements at the time of B_{max} Knop et al. (2003) concluded that the possible reddening of SN 2000fr due to dust in the host galaxy was negligible, (see also Section 6 for a more extensive discussion). The Milky Way reddening is $E(B - V) = 0.030$ mag (Schlegel et al., 1998).

Not Cal Lidman et al
 We always planned extensive follow-up - allow by discovery strategy.

The near-infrared data was collected with ISAAC at the VLT telescope. It consists of J_s -band observations during three epochs and a final reference (see Table 5). Each data point is made of a series of 20 to 60 images with random offsets between exposures. The observations were done in the J_s filter, which is narrower than other J-band filters. Figure 11 shows a comparison between J_s and J Persson filters, together with the atmospheric transmission. Also plotted is the Keck J filter (which is extremely close to the J_s filter).

image of the host galaxy without the SN

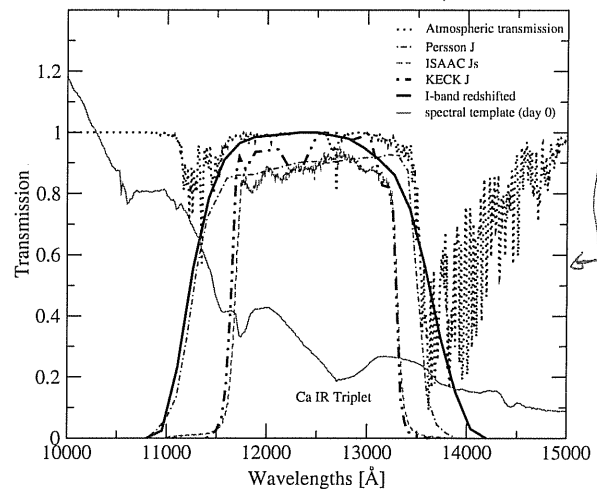


Fig. 11. Comparison between the standard J Persson filter, the J_s filter at ISAAC used for the observations of SN 2000fr and the red shifted I-band. The atmospheric transmission is also plotted. The spectral template at day 0 has been amplified by a factor of 4 for readability of the plot.

It's very hard to find the different lines in this graph

??
 What does it mean to amplify if it looks (flat) are different anyway

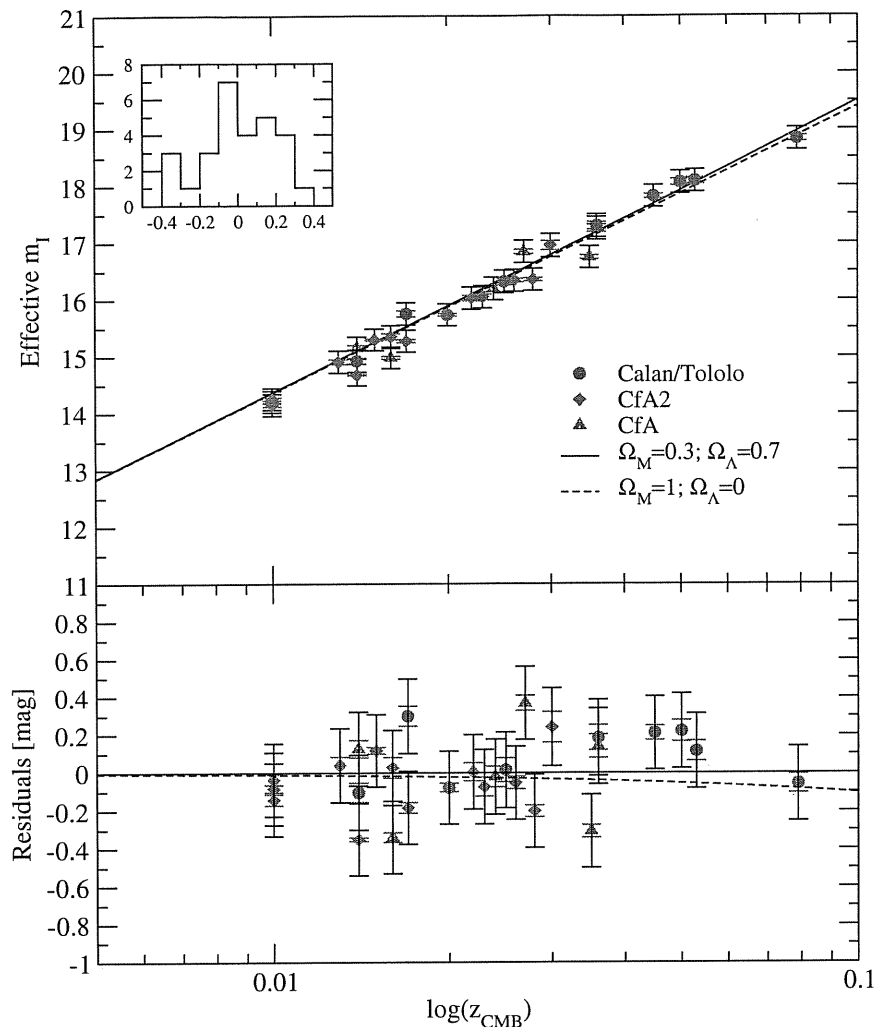


Fig. 10. Effective magnitude I maximum vs redshift for the nearby supernovae of the CT, CfA and CfA2 sample. The data have been corrected for the stretch-luminosity relation and for Milky Way and host galaxy extinction. The r.m.s. along the concordance model line is $\sigma = 0.19 \pm 0.02$ mag.

The advantage in using a narrow J filter is that its transmission function cuts off entirely the region of strong atmospheric absorption between 13500 and 15000 Å. Consequently, the zero-point is significantly more stable than the one of standard J . This was very useful, because all of the ISAAC data was taken in queue mode, where typically only one or two standard stars are observed during a night, chosen from the list of Persson et al. (1998). All data, except the reference images, were taken during photometric nights and the difference in the zero-points from one night to the next were less than 0.01 magnitudes.

The data was reduced using the external package XDIMSUM in IRAF³. The supernova images were aligned with the references and scaled using the field stars before per-

³ IRAF is distributed by the National Optical Astronomy Observatories, which are operated by the Association of Universities for Research in Astronomy, Inc., under cooperative agreement with the National Science Foundation.

| MJD | Epoch | J_s (mag) | I (mag) |
|----------|-------|------------------|------------------|
| 51685.06 | 0.41 | 22.50 ± 0.09 | 23.35 ± 0.09 |
| 51709.02 | 15.94 | 23.57 ± 0.22 | 24.36 ± 0.22 |
| 51731.96 | 30.80 | 23.14 ± 0.15 | 23.93 ± 0.15 |

Table 5. Summary of IR data for SN 2000fr. The quoted errors are due to statistical Poisson noise and uncertainty on the ZP. Epochs are in restframe relative to B -band maximum.

forming PSF photometry. The results are given in Table 5. The stated uncertainties include the statistical Poisson noise and the uncertainty on the estimate of the zero point, add in quadrature.

The J_s -band magnitude takes into account a color term which arises from the difference between the J filter of the standard star system and the J_s filter used in ISAAC. This correction was small ~ 0.012 mag.

The K_{I,J_s} -correction to convert from J_s -band to rest-frame I -band, has been calculated following Kim et al. (1996) using the

cross-filter K -correction,

spectral templates given in Nobili et al. (2003). Given the good match between the observed filter and the restframe one at this redshift, see Figure 11, the uncertainty in the K_{JJ_s} -corrections is dominated by the uncertainty in relating IR and optical photometric systems, which we estimate to be of the order of 0.05 magnitudes.

4.2. SN 1999ff

SN 1999ff was discovered by the High-Z Supernova Search Team (HZT) during a search conducted at CFHT using the CFH-12k camera in *I*-band (Tonry et al., 2003).⁴ The supernova was confirmed spectroscopically as a Type Ia at redshift $z = 0.455$. The Milky Way reddening is $E(B - V) = 0.025$ mag (Schlegel et al., 1998).

J-band observations, corresponding to restframe *I*-band, reported in the paper, were taken at Keck using NIRC in two epochs only. The *J*-band filter available at Keck is also shown in Figure 11, and it is very similar to the ISAAC- J_s . For consistency with the treatment of both the low redshift supernovae and SN 2000fr we computed the K -corrections using the templates in Nobili et al. (2003). The restframe *I*-band magnitudes obtained this way are reported in Table 6. The published optical *R*-band data were used to fit restframe *B*-band lightcurve using the stretch method. The time of maximum was confirmed within 1 day with a best fit for the stretch $s_B = 0.82 \pm 0.05$.

| MJD | Epochs | I(mag) |
|----------|--------|------------------|
| 51501.29 | 6.10 | 23.46 \pm 0.10 |
| 51526.31 | 27.05 | 24.08 \pm 0.24 |

Table 6. Summary of IR data of SN 1999ff. Epochs are in restframe relative to *B*-band maximum ($MJD_{max} = 51494$); restframe *I*-band magnitudes are computed applying K -corrections to the observed *J*-band data published in Tonry et al. (2003).

4.3. SN 1999Q

SN 1999Q was discovered by the HZT using the CTIO 4 m Blanco Telescope, (Riess et al., 2000). It was spectroscopically confirmed to be a Type Ia at redshift $z = 0.46$. The Milky Way reddening is $E(B - V) = 0.021$ mag (Schlegel et al., 1998).

J-band observations were done at 5 different epochs, the first was observed at NTT SOFI and the following epochs at Keck NIRC. The restframe *I*-band computed are given in Table 7.

Restframe *B*-band lightcurve was not reported in the original paper. Thus we could not fit the lightcurve to determine the stretch factor, s_B , nor to confirm the time of restframe *B*-band maximum given in the paper.

⁴ Another supernova, SN 1999fn, was followed in *J*-band by the HZT during the same search. However since it was found in a highly extinguished Galactic field, $E(B-V)=0.32$ mag, and since it was strongly contaminated by the host galaxy, we did not include it in our analysis.

| MJD | Epochs | I(mag) |
|---------|--------|------------------|
| 51204.2 | 6.2 | 23.79 \pm 0.14 |
| 51216.4 | 14.5 | 24.07 \pm 0.17 |
| 51239.3 | 30.2 | 24.44 \pm 0.14 |
| 51243.3 | 32.9 | 24.27 \pm 0.14 |
| 51261.3 | 45.3 | 24.65 \pm 0.19 |

Table 7. Summary of IR data of SN 1999Q. Epochs are in restframe relative to *B*-band maximum; restframe *I*-band magnitudes are computed applying K -corrections using the spectral template in (Nobili et al., 2003) to the observed *J*-band data published in Riess et al. (2000).

4.4. Lightcurve fit of the high-*z* supernovae.

The *I*-band lightcurves of the high redshift supernovae are not well sampled in time as the low redshift sample analyzed in this work. There are only few data points for each SN, making it impossible to perform the 5 parameter fit. Thus, we used the results of the fit of the local sample of supernovae to build a set of *I*-band templates, which in turn have been used to fit the high redshift SN lightcurves.

We performed a one parameter fit, being the amplitude of the maximum, I_{max} , of the 42 templates to the data of the high redshift supernovae. In all the cases we assumed the time of B_{max} to be known from the sources for the published data, and our *B*-band lightcurve fit for SN 2000fr given in Knop et al. (2003). A χ^2 comparison was used to choose the best low-*z* template. In the case of SN 1999Q the data point at day +45 was excluded from the fit for consistency, since only data up to day +40 were used to fit the low redshift lightcurves.

Figs. 12-14 show the comparison of the data with the best fit template for each of the supernovae. Table 8 gives the results of the fit together with redshift, the number of data points, the template giving the best fit and the χ^2 . Given the fact that there are few data points for each SN, the χ^2 parameter has little significance for estimating the goodness of the fits. Thus, to estimate the possible systematic error in the measured peak magnitude from the selection of lightcurve template, we computed the standard deviation from all the lightcurve templates giving a $\chi^2 \leq \chi^2_{min} + 3$. This systematic uncertainty is reported also in Table 8.

4.5. Monte-Carlo test of the fitting method

A Monte-Carlo simulation was run in order to test the fitting method applied to the high-*z* SNe. The uncertainties on the data were used to generate a set of 1000 SNe, randomly distributed around the data points, at the same epochs of the data. All the simulated data sets were in turn fitted with the 42 templates and the one giving the minimum χ^2 was selected for each of the simulation. The distribution of the maximum peak fitted in each of the simulated data sets around the value fitted on the experimental data was studied to check for systematic uncertainty in the fitting procedure. This was found to be robust, always selecting the same template as the one giving the best fit for all the three SNe. No bias was found, therefore confirming the peak magnitude fitted with this method. The uncertainty on

This is interesting - I'm surprised that just 2 or 3 points nail a specific template every time!

we should compare this against our other best spectral templates

I thought that Bohlin gets this down to ~0.03 mag

we should also consider fitting to s_B temp with other priors to average it - there's another way to handle this!

?

| SN | z | n | I_{max} | template | χ^2 | A_J^{MW} |
|-----------|-------|-----|---------------------------|-----------|----------|------------|
| SN 2000fr | 0.543 | 3 | $23.35 \pm 0.07 \pm 0.04$ | SN 1992bc | 0.71 | 0.027 |
| SN 1999ff | 0.455 | 2 | $23.26 \pm 0.10 \pm 0.12$ | SN 1992bc | 0.38 | 0.022 |
| SN 1999Q | 0.460 | 4 | $23.66 \pm 0.07 \pm 0.18$ | SN 1989B | 2.83 | 0.019 |

Table 8. List of the high redshift Type Ia SNe used in this work. Columns are: redshift, number of data points used in the fit, magnitude of the peak resulted from the fit (both statistical and systematic uncertainties are given), best fit template, χ^2 of the fit, Milky Way extinction in the *J*-band.

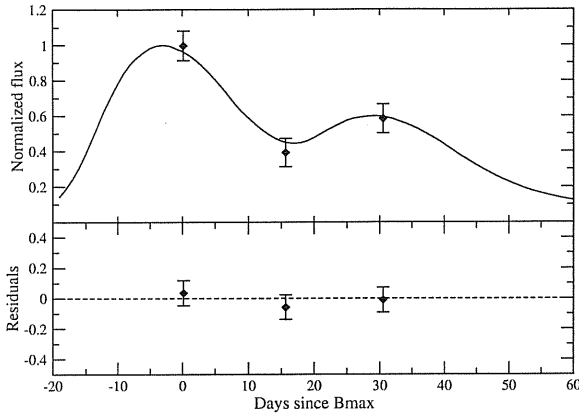


Fig. 12. *I*-band fit for SN 2000fr. Best fit was obtained with the template of the nearby SN 1992bc. The fitted value for the peak is $I_{max} = 23.35 \pm 0.07$ mag.

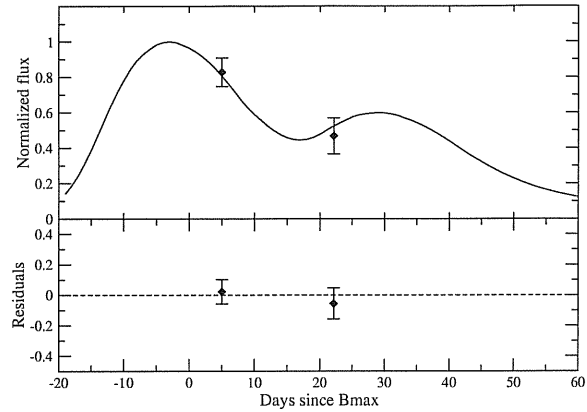


Fig. 14. *I*-band fit for SN 1999ff. Best fit was obtained with the template of SN 1992bc. The fitted value for the peak is 23.26 ± 0.10 mag.

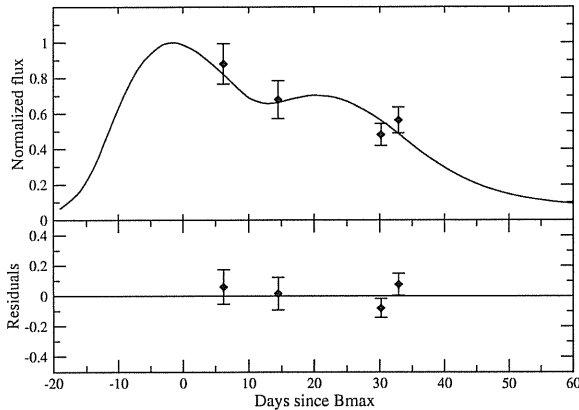


Fig. 13. *I*-band fit for SN 1999Q. Best fit was obtained with the template of SN 1989B. The fitted value for the peak is 23.65 ± 0.07 mag.

I_{max} reported in Table 8 was consistent with the dispersion in the distribution measured on the simulations.

5. The *I*-band Hubble diagram up to $z \sim 0.5$

We want to add the three high redshift SNe in the Hubble diagram. Unfortunately *B*-band data is not available for one of them, SN 1999Q. In order not to treat the SNe differently nor reject 33 % of our sample, we did not apply the width-luminosity relation to correct the *I*-band peak magnitude in our primary analysis of the Hubble diagram, i.e. at the expense of

having a larger dispersion for the local sample, 0.24 mag^5 . The *I*-band peak magnitudes of the high redshift supernovae were thus corrected for Milky Way extinction in the observed band only.

Figure 15 shows the extended Hubble diagram, where an intrinsic uncertainty of 0.24 mag has been added in quadrature to the measurement errors of the plotted data. The solid line represent the best fit to the nearby data for the concordance model $\Omega_M = 0.3$ and $\Omega_\Lambda = 0.7$. Also plotted is the model for $\Omega_M = 1$ and $\Omega_\Lambda = 0$ (dashed line). The low statistics of the high redshift sample is insufficient to draw strong conclusions on cosmological parameters. However a simple χ^2 test would exclude a flat $\Lambda = 0$ universe at 97% confidence level if systematic uncertainties are taken into account or at the 99% confidence level otherwise. The high redshift data were also compared with a flat $\Lambda = 0$ universe in presence of gray dust, $R_V = 9.5$, in the intergalactic medium. The dust density was assumed as such to account for the observed dimming of SNe at $z \sim 0.5$ in *B*-band. Table 9 lists the χ^2 values for the high- z SNe to each of the model. The concordance model results compatible with the data. As a comparison, in the bottom panel of figure 15, we show the residuals obtained if width-luminosity relation corrections are applied. All data have been corrected, except SN 1999Q, for which an intrinsic uncertainty of 0.24 has been added instead of 0.19 considered for the other SNe.

⁵ If we were strictly to consider the intrinsic dispersion as a perfect Gaussian distribution, then it would have been more advantageous to use only 2 supernovae with a sharper “standard candle” width. However, systematic effects cannot be neglected, and using all available SNe is very important in this case

?
Not sure if this meant to say "were thus only corrected"

Re-word

quantity Re-word are consistent

This is a worrying expense — isn't there anything else we can do?

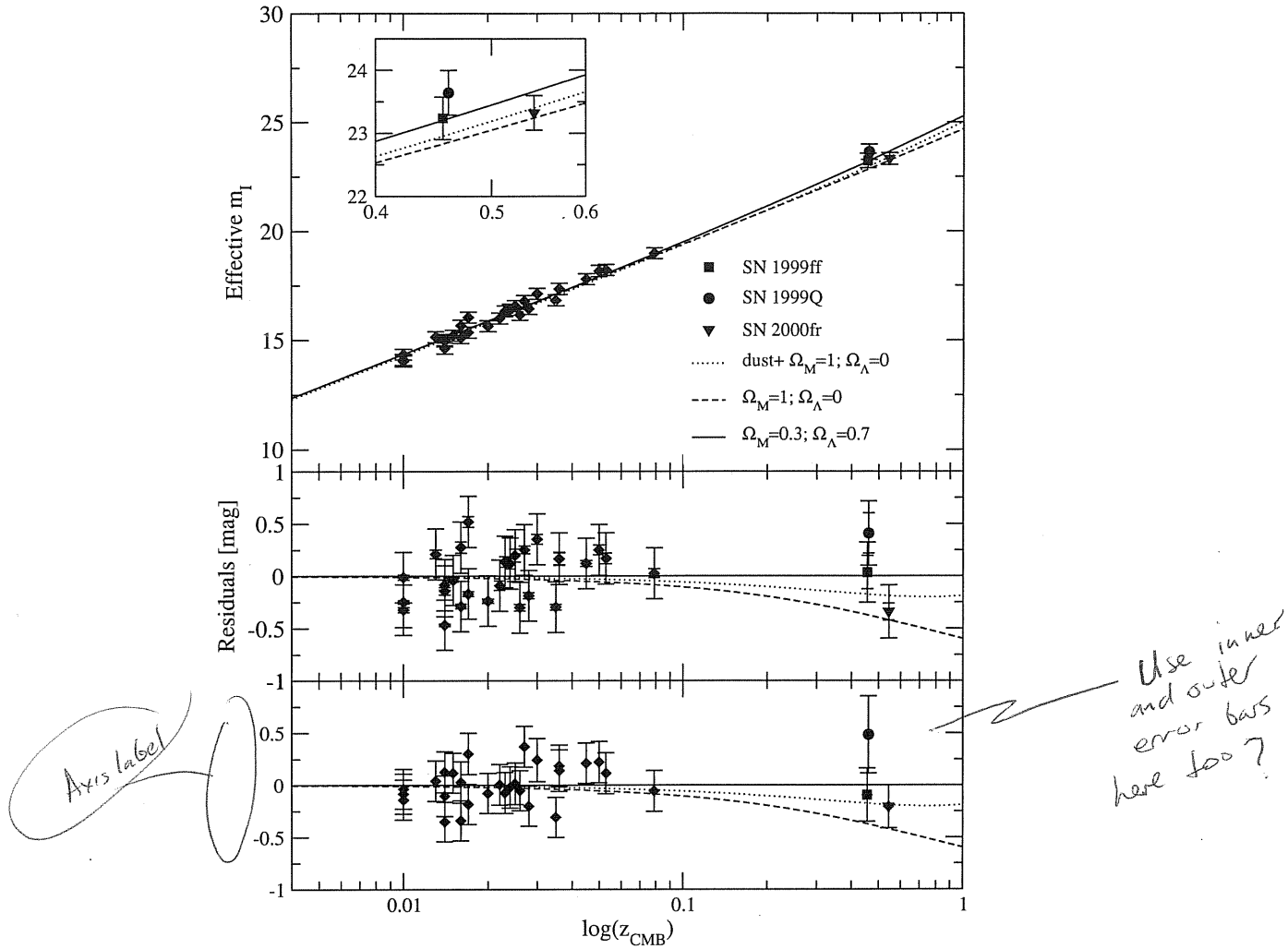


Fig. 15. Effective magnitude *I* maximum vs redshift for the nearby supernovae of the Calan/Tololo, CfA and CfA2 sample, together with three supernovae at redshift ~ 0.5 corrected for Milky Way extinction only. Data not corrected for the width-luminosity relation (top and middle panels) and corrected (bottom panel). Note that the models are the results of a fit to different data in the two cases.

| $(\Omega_M, \Omega_\Lambda)$ | χ_a^2 | χ_b^2 | dof |
|------------------------------|------------|------------|-----|
| (0.3, 0.7) | 3.59 | 4.55 | 3 |
| (1, 0) | 8.61 | 12.4 | 3 |
| (1, 0) _{dust} | 4.51 | 6.51 | 3 |

Table 9. χ^2 of the high redshift data to each model, adding the systematic uncertainties in quadrature (χ_a^2) or neglecting them (χ_b^2).

The scatter between the $z \sim 0.5$ points is 0.38 ± 0.07 mag, i.e. slightly too large to be consistent with the quoted measurement errors. In this sense additional unidentified systematic uncertainties on the distant SNe cannot be excluded.

A general problem concerns *J*-band observations, that correspond to the restframe *I*-band at the redshift considered. Infrared data reduction and calibration remains inferior to what may be achieved at optical wavelengths. Moreover, the standard star systems used are not as well established.

Some uncertainties are specific to the sample considered here. The different fitting methods applied to the restframe *I*-band lightcurve for the low- and high-redshift samples can be easily overcome if distant supernovae are followed at NIR wavelengths with better time coverage. Also both the low-*z* and high-*z* samples used in this analysis are rather heterogeneous, as they were collected from different data sets.

The K-corrections (K_{IJ}) for all SNe were calculated using the spectral template in (Nobili et al., 2003). These differ from the values given in (Tonry et al., 2003; Riess et al., 2000), especially at late time where the disagreement is 0.1-0.2 mag. This is a source of concern, indicating the need for further studies of the properties of the *I*-band part of Type Ia supernova spectrum.

Future homogeneous data sets would naturally solve such kind of problem.

The writing on this page is beginning to ramble a little - could it be tightened up?

Which kind of problem? Not obvious it would solve K-correction

6. SN colors and study on gray dust

Multi-color photometry allows for extinction tests for non-standard dust with only weak wavelength dependence, such as the reddening by a homogeneous population of large grain dust, as proposed by Aguirre (1999a,b). Assuming a density of gray dust in the intergalactic (IG) medium to explain the observed dimming of supernovae at redshift $z = 0.5$ with $\Omega_M = 1$ and $\Omega_\Lambda = 0$, we calculated the expected color extinction following Goobar et al. (2002a) using the SNOC Monte-Carlo package (Goobar et al., 2002b), for two cases of $R_V = 4.5$ and $R_V = 9.5$ and a comoving dust density between $z=0$ and the SN redshifts.

For two of the three SNe considered in this work we computed rest frame $B - V$ and $B - I$. For the third supernova, SN 1999Q, only $B - I$ is available. Table 10 and 11 lists the colors for all the SNe, corrected for Milky Way extinction. The color evolution has been compared to models for a Λ dominated universe and a $\Omega_M = 1, \Omega_\Lambda = 0$ universe with presence of gray dust ($R_V=4.5$ and $R_V=9.5$) accounting for the faintness of Type Ia supernovae at $z \approx 0.5$, and it is shown in Fig. 16. The error bars include also the intrinsic color dispersion contribution.

The reduced χ^2 has been computed to both $B - V$ and $B - I$ evolution and is listed in Table 12. The correlations between SN colors at different epochs found by Nobili et al. (2003) were taken into account. Note that one single SN is not enough to constrain any of the models. The reduced χ^2 computed for the case of SN 1999Q are inconsistent with the constrains on gray dust models given by Riess et al. (2000). The main reasons for the difference is that 1) the authors neglected the possible correlation between colors at different epochs in their calculation, i.e. considered five data points from *one* SN as independent measurements (in this sense Fig. 16 could be misleading since it does not show the correlation between the data belonging to the same SN); 2) they used a different estimate of the intrinsic $B - I$ color.

Are our different models agreed on this?

| day | $B - I$ |
|-----------|------------------|
| SN 2000fr | |
| 0.15 | -0.30 ± 0.09 |
| 14.89 | -0.27 ± 0.22 |
| 28.99 | 1.53 ± 0.15 |
| SN 1999ff | |
| 6.10 | 0.00 ± 0.11 |
| 27.05 | 1.41 ± 0.24 |
| SN 1999Q | |
| 6.20 | -0.45 ± 0.15 |
| 14.50 | -0.05 ± 0.18 |
| 30.20 | 1.17 ± 0.15 |
| 32.90 | 1.51 ± 0.15 |

Table 10. Restframe $B - I$ colors in magnitudes for the three high redshift SNe.

To make our test for gray dust more robust we tried a different approach. The method of least squares (LS) has been used to combine color measurements along time for each supernova,

this could mean many different things here.

| day | $B - V$ |
|-----------|------------------|
| SN 2000fr | |
| -7.35 | -0.17 ± 0.05 |
| -2.98 | -0.14 ± 0.05 |
| 4.99 | -0.09 ± 0.05 |
| 13.16 | 0.26 ± 0.08 |
| 20.42 | 0.61 ± 0.07 |
| 30.15 | 1.01 ± 0.09 |
| SN 1999ff | |
| -7.99 | 0.01 ± 0.08 |
| 1.91 | -0.04 ± 0.09 |
| 1.98 | 0.09 ± 0.12 |
| 2.91 | 0.21 ± 0.12 |
| 19.55 | 0.69 ± 0.09 |
| 28.75 | 1.19 ± 0.20 |

Table 11. Restframe $B - V$ colors in magnitudes for the two of the high redshift SNe.

This is a whole book - is there one page or section, or do you mean the general concept of "least squares"? Also can we explain a little more - or is that what the following sentence is about? Reword

see Cowan (1998) for details. The residuals of each SN colors to the expected model are weighted averaged together, and the covariance matrix is used as weight in the calculation. First we applied this method to all local supernovae and used the results to establish the expected distribution in the $E(B - I)$ vs $E(B - V)$ plane, as showed in Fig. 17. As the high- z SNe were not corrected for host galaxy extinction, we computed the local sample distribution in the two cases: the left panels represent the distribution of color excess of 34 nearby SNe, not corrected (top panel) and corrected (bottom panel) for host galaxy extinction. The amplitude of the ellipses on each axis is given by the estimated standard deviation of the distribution and the inclination is defined by the linear Pearson correlation coefficient computed on the same data sample. The solid line represent 68.3%, the dashed line the 95.5% and the dashed-dotted line the 99.7% probability.

In one dimension or two?

The right panels in Fig. 17 show the combined values of color excess for the high redshift supernovae, where SN 1999Q is represented by a band (horizontal dashed-lines), as the $B - V$ color is missing. These are compared to the local supernova distribution (dotted lines), that represent the distribution expected in the absence of IG dust. Also plotted is the 68.3% level of the expected distribution in presence of "gray" dust with $R_V = 9.5$, represented by the ellipse (dashed line) displaced by (0.06,0.19) from the no-dust model. Only the case of $R_V = 9.5$ has been plotted for readability reasons, given the small difference between the two dust models. The ellipse corresponding to $R_V = 4.5$ would be displaced by (0.09,0.23), respectively in $E(B - V)$ and $E(B - I)$, from the no-dust model.

Remind reader: Explain why the $R_V = 4.5$ model would be further from no-dust?

We computed the χ^2 of the high- z data to each of the models, for both the situation in the top and bottom panels of Figure 17. We add the χ^2 of all the SN to each of the model together, taking into account the correlation found between $E(B - V)$ and $E(B - I)$ in the nearby sample when combining the colors of SN 1999ff and SN 2000fr. The reduced χ^2 (for 5 degrees of freedom) are 2.18, 2.66 and 2.25 for the no-dust, IG dust with $R_V = 4.5$ and IG dust with $R_V = 9.5$ model respectively, for the case corrected for the host-galaxy extinction, corrected case.

Search for use of high- z (and low- z) in the pop and replace with "high- z (and low-redshift")

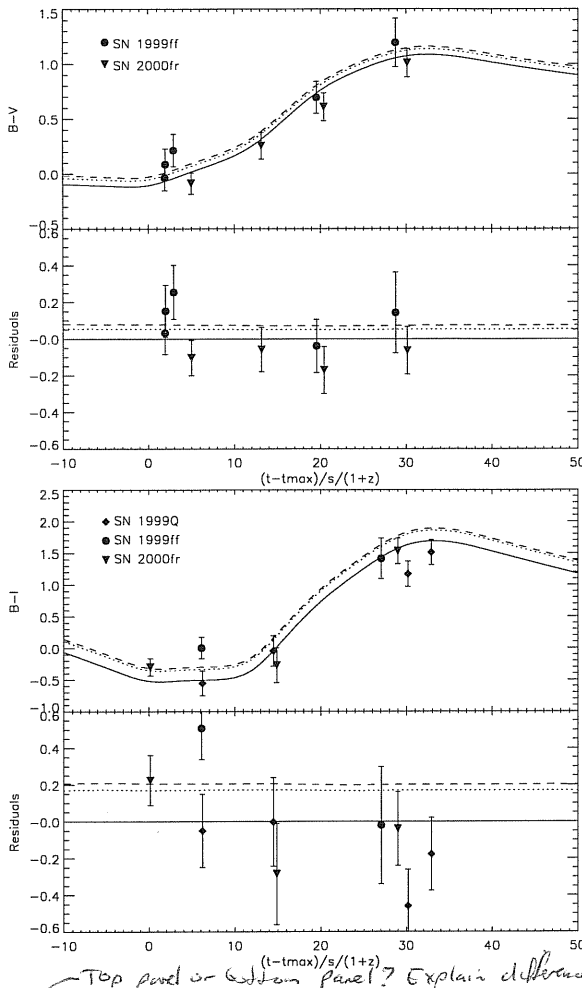


Fig. 16. High redshift SNe color evolution compared to a Λ dominated universe (solid line) and to an $\Omega_M = 1, \Omega_\Lambda = 0$ universe with presence of gray dust with $R_V = 4.5$ (dashed line) and $R_V = 9.5$ (dotted line).

and 1.80, 2.04 and 1.71 otherwise. These results do not allow us to reach any definitive conclusions. A Monte Carlo simulation was used to estimate the minimum sample size needed to test for presence of homogeneously distributed gray dust in the IGM. SNe colors were generated following the binormal distribution defined by the SN local sample. Under the assumption that the systematic effects are negligible and an average measurement uncertainty of 0.05 mag in both $E(B-V)$ and $E(B-I)$, we found that a sample of at least 20 SNe would be needed to be able to exclude the dust models at the 95% C.L.

6.1. Possible systematic effects.

As shown in the previous section, given the data sample available at high redshift it was not possible to draw any firm conclusions about presence of gray dust in the IGM medium. Three data points seem an inadequate (small) sample to be used for a robust statistical analysis. Moreover, the possibility for the result to be affected by systematic effects is not negligible. This becomes clear when looking at the behavior of the single high-z supernova in Figure 16. In particular, the case of SN 1999ff

| | χ^2_{B-V} | χ^2_{B-I} |
|---|----------------|----------------|
| SN 2000fr | | |
| no dust, $(\Omega_M, \Omega_\Lambda) = (0.3, 0.7)$ | 0.52 | 0.81 |
| dust $R_V = 9.5, (\Omega_M, \Omega_\Lambda) = (1, 0)$ | 0.94 | 0.62 |
| dust $R_V = 4.5, (\Omega_M, \Omega_\Lambda) = (1, 0)$ | 1.18 | 0.65 |
| SN 1999ff | | |
| no dust, $(\Omega_M, \Omega_\Lambda) = (0.3, 0.7)$ | 0.87 | 4.87 |
| dust $R_V = 9.5, (\Omega_M, \Omega_\Lambda) = (1, 0)$ | 0.69 | 2.63 |
| dust $R_V = 4.5, (\Omega_M, \Omega_\Lambda) = (1, 0)$ | 0.66 | 2.30 |
| SN 1999Q | | |
| no dust, $(\Omega_M, \Omega_\Lambda) = (0.3, 0.7)$ | — | 2.03 |
| dust $R_V = 9.5, (\Omega_M, \Omega_\Lambda) = (1, 0)$ | — | 2.95 |
| dust $R_V = 4.5, (\Omega_M, \Omega_\Lambda) = (1, 0)$ | — | 3.17 |
| All the SNe combined | | |
| no dust, $(\Omega_M, \Omega_\Lambda) = (0.3, 0.7)$ | 0.71 | 2.26 |
| dust $R_V = 9.5, (\Omega_M, \Omega_\Lambda) = (1, 0)$ | 0.89 | 2.14 |
| dust $R_V = 4.5, (\Omega_M, \Omega_\Lambda) = (1, 0)$ | 0.80 | 2.11 |

Table 12. Reduced χ^2 computed for the 3 different models and colors for each of the supernovae and for all of them combined.

seems worth examining. The first data point of $B-I$ color, lies about two standard deviations above all the models, while the second one lies on top of the curves. This scatter, ~ 0.5 mag, is not justified by the given uncertainties, and is much larger than the intrinsic dispersion measured on nearby supernovae. Note that the problem is not that the SN does not follow the model, but rather the large scatter of the two data points. Table 12 gives the χ^2 values computed for each of the SN to each of the model, and for all of the supernovae combined. In the case of SN 1999ff the χ^2 values for the $B-I$ to each of the model are too large. The same supernova in Figure 17, does not look as extreme, as it is the combination of the two data points shown in Figure 16. The anomaly of this SN does not necessarily indicate that unknown systematic effects are taking place, it may also be the result from possible underestimation of the measurement uncertainties. Increasing the sample and the time sampling for each object would allow us not only to improve the significance of our statistic, but it will also be a mean to identify and quantify systematic effects involved.

7. Test for SN brightness evolution

Evolution of the properties of the supernova progenitors with redshift has been often proposed as an alternative explanation to the observed dimming of distant SNe. This is based on the fact that older galaxies show different composition than younger ones, e.g. an increased metallicity, therefore offering different environmental conditions to the exploding star. A simple way to test for evolution is to compare properties of nearby SNe with distant ones. This will not prove that there is no evolution, but it will exclude it on a supernova-by-supernova or property-by-property basis, finding always counterparts of distant events in the local sample.

In this work we compared colors of nearby and distant supernovae (primarily to test presence of "gray" dust). Although the size of the high redshift sample is very limited, our attempt does not give evidence for evolution of the average SN col-

The difference between absolute chi-squares, not reduced chi-squares (if this is what is meant here)
 important point (I think): Comparing models should be done with uncorrected
 Top panel or bottom panel? Explain difference
 which? - there is not just one single high-redshift SN. Do you mean "any single"

with best extinction or without - top or bottom pane
 No? quanti
 How can you tell which is problem

How we this underest. occur
 distributions

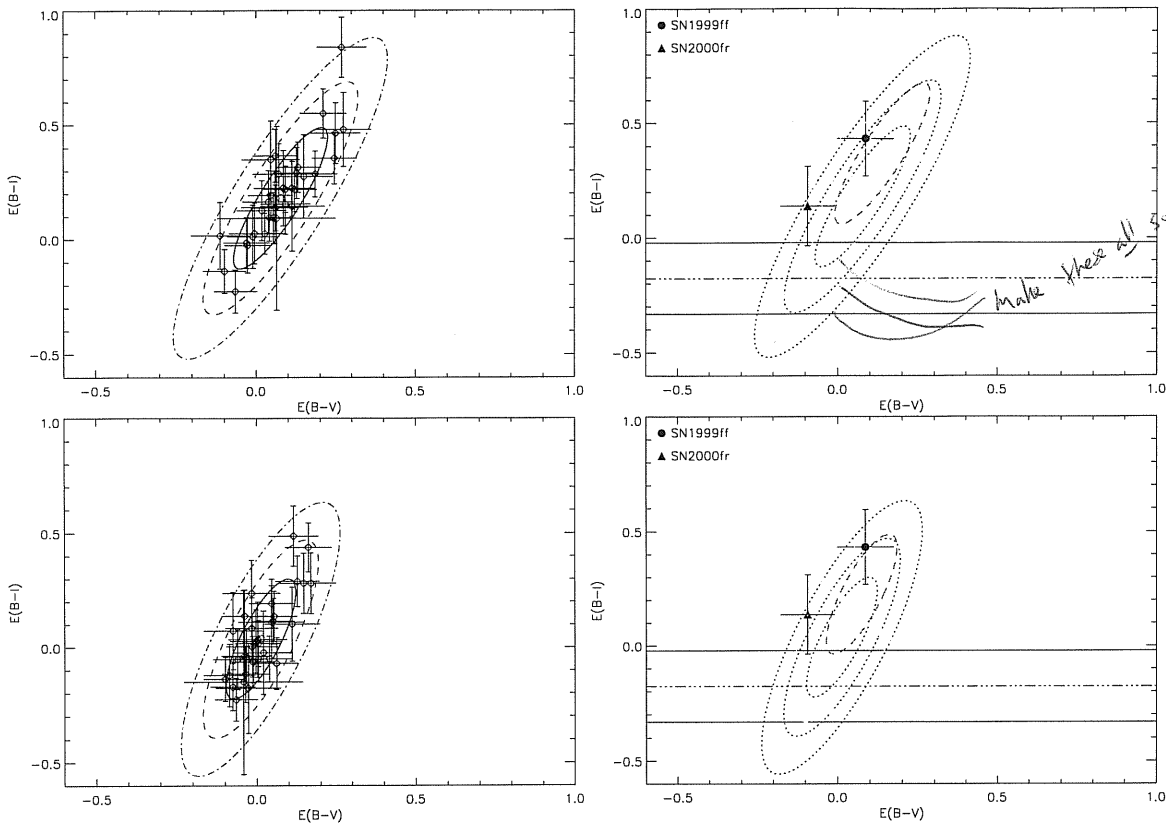


Fig. 17. Left panels: distribution of combined color measurements for the local sample of supernovae in the $E(B - I)$ vs $E(B - V)$ plane, not corrected (top panel) and corrected (bottom panel) for the host galaxy extinction. The solid line is the 68.3%, the dashed line the 95.5%, and the dashed-dotted line the 99.7% of probability. Right panels: combined colors of the high redshift supernovae compared to the distribution in the absence of IG dust (dotted ellipses), and the one expected in presence of gray dust in the IG medium with $R_V = 9.5$ (dashed ellipse). SN 1999Q is represented by an horizontal solid line band, as the $B - V$ color is missing, SN 1999ff by the filled circle and SN 2000fr by the filled triangle. For simplicity only the 68.3% level has been plotted for the dust distribution.

| | <i>n</i> | SN 1991bg | SN 1997cn |
|-----------|----------|-----------|-----------|
| SN 2000fr | 3 | 24.21 | 25.24 |
| SN 1999ff | 2 | 1.98 | 1.62 |
| SN 1999Q | 4 | 36.72 | 36.57 |

Table 13. $\Delta\chi^2$ for the fit of the high-*z* SNe to the templates of the two sub-luminous SNe. *n* is the number of data points used in the one-parameter fit (see discussion in section 4.4).

relative to the best fits (which are the "normal" SN templates)

ors. Furthermore, the correlation found between the intensity of the secondary peak of *I*-band lightcurve and the supernova luminosity give an independent way of testing for evolution. The restframe *I*-band lightcurve for the high-redshift supernovae were all fitted by templates showing a prominent second peak, i.e. inconsistent with the intrinsically underluminous supernovae necessary to explain the apparent faintness of high-*z* supernovae in a flat $\Lambda = 0$ universe. Note that, for at least one supernova, SN 2000fr, the secondary peak is evident on the data even prior the lightcurve is fitted. Table 13 lists the $\Delta\chi^2$ for the fit of the high-*z* SNe to the templates of the two sub-luminous SN 1991bg and SN 1997cn, relative to the best fit. The χ^2 values are significantly larger than the best fit value.

8. Summary and conclusions

In this work we have investigated the feasibility of using restframe *I*-band observations for cosmological purposes.

We have developed a five parameter lightcurve fitting procedure which was applied successfully to 42 nearby Type Ia supernovae. The fitted lightcurves were used to build a set of templates which include a broad variety of shapes. We have found correlations between the fitted parameters, in particular between the time of the secondary peak and the *B*-band stretch, s_B , as well as the *I*-band stretch, s_I . Moreover, a width-luminosity relation was found for the *I*-band peak magnitude.

We built a restframe *I*-band Hubble diagram using 28 nearby supernovae at redshifts $0.01 \leq z \leq 0.1$, and measured a dispersion of 0.24 ± 0.02 mag, smaller than the uncorrected dispersion corresponding to restframe *B*-band. The width-luminosity relation was used to reduce the dispersion to 0.19 ± 0.02 mag. This dispersion differs for each of the three data samples, ~ 0.15 in both the Calan/Tololo and CfA2 samples and ~ 0.28 in the CfA sample.

I-band measurements of three high redshift supernovae were used to extend the Hubble diagram up to $z \sim 0.5$. Their restframe *I*-band lightcurve was fitted by the template set built

I'm a little bit surprised by this result, since you wouldn't think the data for 99ff and 99Q could tell that there are two peaks. What makes these χ^2 worse (especially why 99Q so much worse)? Are there particularly important constraints?

on the local SNe sample, as the five parameter fit method could not be used for the poorly sampled high-*z* lightcurve.

The data is found compatible with the “concordance model” of the universe, $(\Omega_M, \Omega_\Lambda) = (0.3, 0.7)$. A flat, $\Lambda = 0$ universe is excluded at the 99% confidence level.

Alternative explanations of the observed dimming of supernova brightness, such as presence of gray dust in the IG medium or evolution effects in the supernova properties have also been addressed. Both the *I*-band Hubble diagram and multi color photometry have been used for testing gray dust. Preliminary results based on only three high-*z* supernovae in the Hubble diagram disfavor the gray dust hypothesis at the 90% confidence level. The results obtained using color diagrams were less significant, the data being compatible with both dust and no-dust color distributions. However, a Monte Carlo simulation indicates that a sample of at least 20 well observed SNe would be enough for testing the presence of a homogeneous dust distribution in the IGM, using only the color diagram technique.

Possible systematic uncertainties affecting the restframe *I*-band Hubble diagram are discussed. Some sources are identified, for instance the different methods applied for fitting the low and the high-redshift samples, selection effects for bright objects during the search campaign, uncertainties connected with the *J*-band data calibration, as well as uncertainties in the *K*-correction calculations due to the presence of the Ca IR triplet feature in the near infrared region of the SN spectra. However, these systematic uncertainties differ from the ones that could affect the restframe *B*-band Hubble diagram. Thus the use of *I*-band measurements of Type Ia supernovae, and the methods developed in this work for testing both cosmological models or its alternative, are showed to be quite robust, and can be complementary to the already well established means.

Acknowledgements. S.N. is supported by a graduate student grant from the Swedish Research Council.

References

- Garavini, G. et al. 2003 (in prep)
- Goldhaber, G., Groom, D. E., Kim, A. et al., 2001, ApJ, 558, 359G
- Goobar, A., Bergström, L. & Mörtzell, E., 2002, A&A, 384, 1.
- Goobar, A., Mörtzell, E., Amanullah, R., Goliath, M., Bergström, L. & T. Dahlen, 2002, A&A, 392, 757.
- Hamuy, M., Phillips, M.M., Suntzeff, N.B. et al. 1996, AJ, 112, 2408
- Hamuy, M., Phillips, M.M., Suntzeff, N.B. et al. 1996, AJ, 112, 2398H
- Henry J. P. 2001, ApJ 534, 565
- Howell, D.A, 2001, ApJ, 554, 193
- Jaffe, A.H., Ade, P.A., Balbi, A. et al., 2001, Phys. Rev. Lett. 86, 3475
- Jha, S., 2002, PhD thesis, Harvard University.
- Kim, A., Goobar, A. & Perlmutter, S., 1996, PASP, 108, 190
- Knop, R. et al. 2003, submitted
- Krisciunas, K., Phillips, M.M., Stubbs, C. et al., 2001, AJ, 122, 1616K
- Leibundgut, B., Kirshner, R. P., Phillips, M.M. et al., 1993, AJ, 105, 301.
- Li, W., Filippenko, A.V. & Treffers, R.R., 2001, ApJ, 546, 734
- Maza, J., Hamuy, M., Phillips, M., Suntzeff, N. & Aviles, R., 1994, ApJ, 424, L107
- Mörtzell, E., Bergström, L. and Goobar, A., 2002, Phys. Rev. D66, 047702.
- Nobili, S., Goobar, A., Knop, R., & Nugent, P., 2003, A&A 404, 901-912
- Nugent P., Kim A. & Perlmutter S., 2003, PASP 114, 803
- Perlmutter, S., Aldering, G., Goldhaber, G. et al., 1999, ApJ, 517, 565
- Persson, S.E., Murphy, D.C., Krzeminski, W., Roth, M. & Rieke, M.J., 1998 A.J. 116, 2475.
- Phillips, M.M., Lira, P., Suntzeff, N.B., Schommer, R.A., Hamuy, M. & Maza, J., 1999, AJ, 118:1766-1776
- Richmond, M.W., Treffers, R.R., Filippenko, A.V. et al. 1995, AJ 109, 2121
- Riess, A., et al. 1998, AJ, 116, 1009.
- Riess, A.G., Filippenko, A.V., Challis, P. et al. 1999, ApJ. 117, 707-724
- Riess, A.G., Filippenko, A.V., Liu, M.C. et al., 2000, ApJ. 536, 62-67
- Rowan-Robinson, M., 2002, MNRAS, 332, 352.
- Schlegel, D.J., Finkbeiner, D.P. & Davis, M. 1998, ApJ, 500, 525S
- Sievers, J.L., Bond, J.R., Cartwright, J.K. et al., 2003, ApJ, 591, 599
- Spergel, D.N., Verde, L., Peiris, H.V. et al., 2003, ApJS, 148, 175S
- Tonry, J.L., Schmidt B.P., Barris, B. et al 2003, astro-ph/0305008
- Wang, L., Goldhaber, G., Aldering, G., Perlmutter, S. 2003, ApJ, 590, 944
- Wells, L.A., Phillips, M.M., Suntzeff, B. et al., 1994 AJ 108, 2233
- Aguirre, A. 1999, ApJ, 512, L19
- Aguirre, A. 1999, ApJ, 525, 583
- Balbi, A., Ade, P., Bock, J. et al., 2000, ApJ, 545, L1.
- Borgani, S., Rosati, P., Tozzi, P. et al. 2001, ApJ, 561, 13
- Cardelli, J. A, Clayton, G.C. & Mathis, J.S. 1989, ApJ, 345, 245
- Contardo, G., Leibundgut, B. & Vacca, W. D. 2000, A&A , 359, 876C
- Cowan, G., 1998, Statistical data analysis, Oxford University Press
- C. Csaki, N. Kaloper & J. Terning, hep-ph/0111311.
- De Bernardis, P., Ade, P.A.R., Bock, J.J. et al., 2000, Nature, 404, 955
- C. Deffayet, D. Harari, J. P. Uzan & M. Zaldarriaga, hep-ph/0112118.
- Drell, P., Lored, T. & Wasserman, I., 2000, ApJ, 530, 593.
- Efstathiou, G., Moody, S., Peacock, J.A. et al, 2002, MNRAS, 330, L29.
- Filippenko, A.V., Richmond, M.W., Branch, D. et al., 1992, AJ, 104, 1543

Don't forget full acknowledgment list, including telescopes that contributed to

SN 200fr.